# Cationic Silver Coordination Compounds of Polydentate Ligands: Supramolecular Structures of $[Ag(Pz^{bp2}Py)_2(OSO_2CF_3)]$ and $[Ag_2(Pz^{bp2}Py)_2(OSO_2CF_3)_2]$ {$Pz^{bp2}Py$ = 2-[3,5-Bis(4-butoxyphenyl)pyrazol-1-yl]pyridine}

**M. Luz Gallego,[a] Mercedes Cano,*[a] José A. Campo,[a] José V. Heras,[a] Elena Pinilla,[a,b] M. Rosario Torres,[b] Pilar Cornago,[c] and Rosa M. Claramunt*[c]**

**Keywords:** N ligands / NMR spectroscopy / Silver / Supramolecular chemistry

The new silver complexes $[Ag(Pz^{bp2}Py)_2(OSO_2CF_3)]$, $[Ag_2(Pz^{bp2}Py)_2(OSO_2CF_3)_2]$, $[Ag(Pz^{bp}Py)_2(OSO_2CF_3)]$, $[Ag_3(TPz^{bp2}Tz)(OSO_2CF_3)_3]$ and $[Ag_3(TPz^{bp}Tz)(OSO_2CF_3)_3]$ (**5**–**9**) have been obtained by reaction of $Ag(OSO_2CF_3)$ with the corresponding polydentate ligand 2-[3,5-bis(4-butoxyphenyl)pyrazol-1-yl]pyridine ($Pz^{bp2}Py$, **1**), 2-[3-(4-butoxyphenyl)pyrazol-1-yl]pyridine ($Pz^{bp}Py$, **2**), 2,4,6-tris[3,5-bis(4-butoxyphenyl)pyrazol-1-yl]-1,3,5-triazine ($TPz^{bp2}Tz$, **3**) and 2,4,6-tris[3-(4-butoxyphenyl)pyrazol-1-yl]-1,3,5-triazine ($TPz^{bp}Tz$, **4**), respectively. The coordination effects induced on the $^1H$, $^{13}C$ and $^{15}N$ NMR chemical shifts of the complexes in solution and in the solid state have been quantified, with the $^{15}N$ NMR spectra being used as a tool to establish the coordination site. All complexes are consistent with an *N*,*N*′-chelating coordination at each silver centre involving nitrogen atoms from pyrazole and pyridine groups for **5** and **7** or from pyrazole and triazine groups for **8** and **9**. An additional Ag···$OSO_2CF_3$ interaction completes the environment around the silver atom, giving rise to a five-coordination or a three-coordination for complexes **5** and **7** and **8** and **9**, respectively. The X-ray structures of **5** and **6** confirm the presence of the *N*,*N*′-chelating coordination of the $Pz^{bp2}Py$ ligands and the coordinative participation of the $CF_3SO_3$ counterion in the metal environment. The Ag···$\eta^2$-arene bonds between neighbouring units in **6** are responsible for the dimers containing four-coordinate silver atoms. At a supramolecular level, Ag···O, C–H···O or C–H···F interactions generate a 2D network in both compounds.



## Introduction

Cationic silver(I) coordination compounds containing N-donor ligands have extensively been described as producing supramolecular arrays of different dimensionality in the solid, this fact being related with the coordinative versatility of the silver atom to adopt several coordination numbers and with the variety of N-donor ligands and counterions.[1,2]

In previous papers we began to study the molecular assemblies produced by silver or gold coordination to substituted pyrazole ligands ($HPz^{R2}$). The cationic coordination compounds containing monodentate $HPz^{R2}$ ligands [$HPz^{R2}$ = 3,5-bis(butoxyphenyl)pyrazole ($HPz^{bp2}$), 3,5-dimethyl-4-nitropyrazole ($HPz^{NO_2}$)] were bonded to their respective counterions, $NO_3^-$, $BF_4^-$ or $CF_3SO_3^-$, giving rise to 1D, 2D and 3D networks through hydrogen-bonding interactions between the counterion and the cationic fragment. Hydrogen bonds involving the H-atom of the pyrazole ligand and some other non-classical hydrogen-bonding interactions were responsible for the networks of different dimensionality.[3–5]

On this basis, we thought that related polydentate ligands based on the pyridine or triazine cores and pyrazole groups as substituents (in which the NH is absent) should be candidates for supramolecular arrays of metallic complexes centred on coordinative bonds or coordinative interactions. There are several examples described in the literature of supramolecular networks based on a silver centre and different types of N-donor ligands.[1,6]

We present here our studies of new silver complexes containing the polydentate ligands 2-[3,5-bis(4-butoxyphenyl)-pyrazol-1-yl]pyridine ($Pz^{bp2}Py$, **1**), 2-[3-(4-butoxyphenyl)pyrazol-1-yl]pyridine ($Pz^{bp}Py$, **2**), 2,4,6-tris[3,5-bis(4-butoxyphenyl)pyrazol-1-yl]-1,3,5-triazine ($TPz^{bp2}Tz$, **3**) and 2,4,6-tris[3-(4-butoxyphenyl)pyrazol-1-yl]-1,3,5-triazine ($TPz^{bp}Tz$, **4**; Scheme 1). The silver compounds **5**–**9** were obtained by treatment of $Ag(OSO_2CF_3)$ with the respective polydentate ligand. These new complexes exhibit variable environments around the metal centre in which the nitrogen atoms of the

[a] Departamento de Química Inorgánica I, Facultad de Ciencias Químicas, Universidad Complutense,
28040 Madrid, Spain
Fax: +34-91-394-4352
E-mail: mmcano@quim.ucm.es
[b] Laboratorio de Difracción de Rayos-X, Facultad de Ciencias Químicas, Universidad Complutense,
28040 Madrid, Spain
[c] Departamento de Química Orgánica y Bio-Orgánica, Facultad de Ciencias, UNED,
28040 Madrid, Spain

Supporting information for this article is available on the WWW under http://www.eurjic.org or from the author.

polydentate PzPy and PzTz units and the oxygen atoms from the counterion $CF_3SO_3^-$ are involved. In particular, an additional Ag···$\eta^2$-arene interaction is also established for **6** (Scheme 2). The structures of the complexes are supported by multinuclear magnetic resonance studies and, in the cases of **5** and **6**, by X-ray crystallography. Formation of one- and multidimensional networks through the interconnection of metallic centres by the inorganic $CF_3SO_3^-$ anion, as well as coordinative Ag···O and Ag···$\eta^2$-arene and other non-coordinative C–H···F, C–H···O, or π···π interactions, will be discussed.

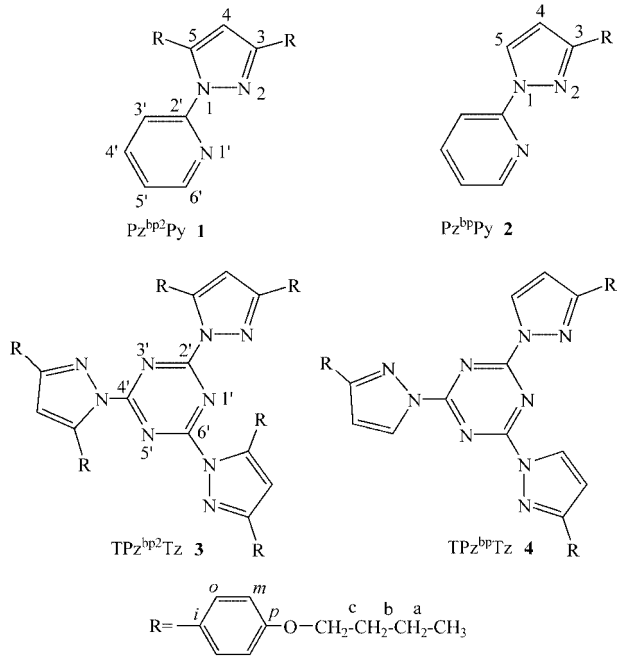


Scheme 1. Polydentate ligands used in this work, with the atomic numbering used for the NMR discussion.

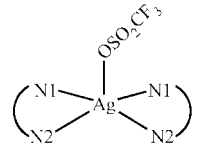


$[Ag(Pz^{bp2}Py)_2(OSO_2CF_3)]$ **5**
$[Ag(Pz^{bpPy})_2(OSO_2CF_3)]$ **7**

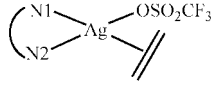


$[Ag_2(Pz^{bp2}Py)_2(OSO_2CF_3)_2]$ **6**

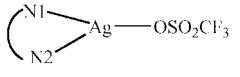


$[Ag_3(TPz^{bp2}Tz)(OSO_2CF_3)_3]$ **8**
$[Ag_3(TPz^{bpTz})(OSO_2CF_3)_3]$ **9**

N1 = nitrogen of the pyrazole group
N2 = nitrogen of the pyridyl or triazine group

Scheme 2. The complexes and their corresponding coordination environments described in this work.

## Results and Discussion

### Syntheses of Ligands and Silver(I) Complexes

The synthesis of 2-[3-(4-butoxyphenyl)pyrazol-1-yl]pyridine ($Pz^{bp}Py$, **2**) and 2,4,6-tris[3-(4-butoxyphenyl)pyrazol-1-yl]-1,3,5-triazine ($TPz^{bp}Tz$, **4**) was achieved by reaction of the sodium salt of 3-(4-butoxyphenyl)propane-1,3-dione with hydrazinopyridine and the sodium salt of 3-(4-butoxyphenyl)pyrazole with 2,4,6-trichlorotriazine, respectively, by similar procedures to those of the related compounds 2-[3,5-bis(4-butoxyphenyl)pyrazol-1-yl]pyridine ($Pz^{bp2}Py$, **1**) and 2,4,6-tris[3,5-bis(4-butoxyphenyl)pyrazol-1-yl]-1,3,5-triazine ($TPz^{bp2}Tz$, **3**) previously described by us.[4,7]

Silver complexes **5**–**9** were obtained by combining the inorganic salt $Ag(OSO_2CF_3)$ with ligands **1**–**4** in different stoichiometries, giving rise to monometallic $[Ag(Pz^{bp2}Py)_2(OSO_2CF_3)]$ (**5**) and $[Ag(Pz^{bp}Py)_2(OSO_2CF_3)]$ (**7**) (from 1:2), dimetallic $[Ag_2(Pz^{bp2}Py)_2(OSO_2CF_3)_2]$ (**6**) (from 1:1) or trimetallic $[Ag_3(TPz^{bp2}Tz)(OSO_2CF_3)_3]$ (**8**) and $[Ag_3(TPz^{bp}Tz)(OSO_2CF_3)_3]$ (**9**) (from 3:1) complexes. Scheme 2 shows the molecular characteristics of the three types of compounds. A more detailed description of trimetallic complexes **8** and **9** is given in Scheme 3.

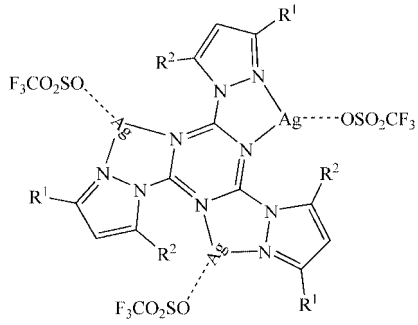


$[Ag_3(TPz^{bp2}Tz)(OSO_2CF_3)_3]$ **8** $R^1 = R^2 = C_6H_4OC_4H_9$

$[Ag_3(TPz^{bp}Tz)(OSO_2CF_3)_3]$ **9** $R^1 = C_6H_4OC_4H_9$; $R^2 = H$

Scheme 3. Schematic representation of trimetallic compounds **8** and **9**.

The IR spectra of the new complexes **5**–**9** were recorded in KBr in the 4000–400 $cm^{-1}$ range. For comparative purposes, the IR spectra of the free ligands were also obtained. The new complexes exhibit the characteristic bands of the ligands, slightly modified by coordination. Compounds **5** and **6** were also characterised by X-ray diffraction and show Ag–O distances of 2.704(8) and 2.325(6) Å, respectively, as will be described below. The former one could be considered to be a coordinative Ag···O interaction[1c,1f,1g,1i,1l,1m,6a,8] or even an Ag–O bond, as has been reported by some authors,[1h,1m,9] whereas the latter is clearly characteristic of an Ag–O bond.[1i,1k,10] The IR spectra of **5** and **6** show absorption frequencies at 1273 and

  

1288 $cm^{-1}$, respectively, assigned to $\nu_{as}(SO_3)$.[11] Thus, the $\nu_{as}(SO_3)$ values for related compounds are tentatively used to differentiate between interactions and/or covalent bonds. Following these results, the $\nu_{as}(SO_3)$ absorption at 1290 $cm^{-1}$ in **8** suggests a strong Ag···O interaction. The related complex **9** exhibits a broad band centred at 1253 $cm^{-1}$, characteristic of the ligand, which could mask the $\nu_{as}(SO_3)$ absorption.

### Multinuclear Magnetic Resonance Spectroscopy

The $^1H$ NMR spectroscopic data of the ligands and their complexes are gathered in Tables 1 and 2.

The $^1H$ NMR spectra of $[Ag(Pz^{bp2}Py)_2(OSO_2CF_3)]$ (**5**) and $[Ag_2(Pz^{bp2}Py)_2(OSO_2CF_3)_2]$ (**6**) show all the expected resonances of the $Pz^{bp2}Py$ units. In both cases, as expected, an inequivalence of the substituents at the 3- and 5-positions of the pyrazole ring is observed, in agreement with the lack of symmetry. This fact is reflected by the presence of two sets of signals for the $OCH_2$ groups and the aromatic $H_o$ and $H_m$ protons of the substituents. In solution, the two $Pz^{bp2}Py$ ligands appear to be equivalent in both complexes, as deduced from the unique signals observed for the H4 proton and the pyridine protons. The signals of the latter ones are shifted downfield in relation to the free ligand (specially noted in **6**), except the H3′ signal, which is shifted upfield by about 0.5 ppm. In contrast, the environment of the aromatic $C_6H_4$ protons is not significantly modified, thus indicating that metal–arene interactions do not exist in solution.[2e,2f,12]

When comparing the $^1H$ NMR spectra of $[Ag(Pz^{bp}Py)_2(OSO_2CF_3)]$ (**7**) with that of **5**, very close chemical shifts are observed for the signals of the pyridine protons H5′ and H6′, whereas for the signals of H3′ and H4′ the shift upon complexation is larger in complex **5**.

Complexes $[Ag_3(TPz^{bp2}Tz)(OSO_2CF_3)_3]$ (**8**) and $[Ag_3(TPz^{bp}Tz)(OSO_2CF_3)_3]$ (**9**) present analogous $^1H$ NMR spectra, the only differences coming from the pyrazole moieties. This fact suggests similar three-coordinate silver environments by considering the chelating complexation through the nitrogen atoms of the pyrazole and triazine rings (N-Pz and N-Tz) and the Ag···$OSO_2CF_3$ interaction proposed above from their IR spectra. Complex **8** exhibits two different types of signals for the aromatic protons $H_o$ and $H_m$, the first set is broad and the second one shows sharp multiplets. An analogous behaviour is found for the 4-butoxyphenyl substituent in complex **9**. The broadness of the signals in both complexes can be explained on the basis

Table 1. $^1H$ NMR chemical shifts ($\delta$ in ppm) and coupling constants ($J$ in Hz) of the pyrazole moiety in compounds **1**–**9**.[a]

| Compound<br>Solvent<br>(pyrazole moiety) | $^aCH_3$ | $^bCH_2$ | $^cCH_2$ | $OCH_2$ | $H_m$ | $H_o$ | H4 | H5 |
|---|---|---|---|---|---|---|---|---|
| **1** | 0.98 (t) | 1.51 (m) | 1.78 (m) | 3.97 (t) | 6.84 (m) | 7.21 (m) | 6.71 (s) | |
| $CDCl_3$ | $^3J$ = 7.4 | | | $^3J$ = 6.5 | | | | |
| ($Pz^{bp2}$) | 0.99(t) | | | 4.01 (t) | 6.95 (m) | 7.86 (m) | | |
| | $^3J$ = 7.4 | | | $^3J$ = 6.5 | | | | |
| **2** | 0.99 (t) | 1.51 (m) | 1.80 (m) | 4.01 (t) | 6.84 (m) | 7.85 (m) | 6.71 (d) | 8.57 (d) |
| $CDCl_3$ | $^3J$ = 7.4 | | | $^3J$ = 6.5 | | | $^3J$ = 2.6 | $^3J$ = 2.6 |
| ($Pz^{bp}$) | | | | | | | | |
| **3** | 0.94 (t) | 1.43 (m) | 1.72 (m) | 3.87 (t) | 6.85 (m) | 7.24 (m) | 6.63 (s) | |
| $CDCl_3$ | $^3J$ = 7.4 | | | $^3J$ = 6.6 | | | | |
| ($Pz^{bp2}$) | 1.01 (t) | 1.51 (m) | 1.82 (m) | 4.04 (t) | 6.98 (m) | 7.76 (m) | | |
| | $^3J$ = 7.4 | | | $^3J$ = 6.5 | | | | |
| **4** | 1.00 (t) | 1.51 (m) | 1.79 (m) | 4.00 (t) | 6.97 (m) | 7.91 (m) | 6.77 (d) | 8.71 (d) |
| $CDCl_3$ | $^3J$ = 7.4 | | | $^3J$ = 6.5 | | | $^3J$ = 2.9 | $^3J$ = 2.9 |
| ($Pz^{bp}$) | | | | | | | | |
| **5** | 0.93 (t) | 1.40 (m) | 1.66 (m) | 3.77 (t) | 6.67 (m) | 7.64 (m) | 6.76 (s) | |
| $CD_2Cl_2$ | $^3J$ = 7.4 | | | $^3J$ = 6.5 | | | | |
| ($Pz^{bp2}$) | 1.00 (t) | 1.53 (m) | 1.81 (m) | 4.04 (t) | 6.98 (m) | 7.28 (m) | | |
| | $^3J$ = 7.4 | | | $^3J$ = 6.5 | | | | |
| **6** | 0.92 (t) | 1.29–1.88 (m) | 1.29–1.88 (m) | 3.79 (t) | 6.76 (d) | 7.35 (d) | 6.98 (s) | |
| $CD_3COCD_3$ | $^3J$ = 7.3 | | | $^3J$ = 6.3 | $^3J$ = 8.8 | $^3J$ = 8.8 | | |
| ($Pz^{bp2}$) | 1.00 (t) | | | 4.09 (t) | 7.06 (d) | 7.76 (d) | | |
| | $^3J$ = 7.3 | | | $^3J$ = 6.3 | $^3J$ = 8.8 | $^3J$ = 8.8 | | |
| **7** | 0.96 (t) | 1.46 (m) | 1.72 (m) | 3.88 (t) | 6.67 (m) | 7.72 (m) | 6.94 (d) | 8.51 (d) |
| $CD_2Cl_2$ | $^3J$ = 7.4 | $^3J$ = 7.5 | $^3J$ = 7.0 | $^3J$ = 6.5 | | | $^3J$ = 2.8 | $^3J$ = 2.8 |
| ($Pz^{bp}$) | | | | | | | | |
| **8** | 0.93 (t) | 1.41 (br) | 1.67 (br) | 3.85 (br) | 7.01 (m) | 7.46 (m) | 6.67(s) | |
| $CDCl_3$ | $^3J$ = 6.9 | | | | | | | |
| ($Pz^{bp2}$) | 1.03 (t) | 1.55 (br) | 1.83 (br) | 4.04 (br) | 7.14 (br) | 7.71 (br) | | |
| | $^3J$ = 6.6 | | | | | | | |
| **9** | 0.90 (t) | 1.38 (br) | 1.62 (br) | 3.88 (br) | 6.88 (br) | 7.88 (br) | 7.05 (br) | 9.10 (br) |
| $CD_3COCD_3$ | $^3J$ = 7.2 | | | | | | | |
| ($Pz^{bp}$) | | | | | | | | |

[a] See Scheme 1 for numbering.

  

Table 2. $^1$H NMR chemical shifts ($\delta$ in ppm) and coupling constants ($J$ in Hz) of the pyridine nucleus in compounds **1**, **2** and **5**–**7**.[a]

| Compound<br>Solvent | H3′ | H4′ | H5′ | H6′ |
|---|---|---|---|---|
| **1** | 7.50 (d) | 7.70 (ddd) | 7.19 (m) | 8.41 (m) |
| $CDCl_3$ | $^3J$ = 8.1 | $^3J$ = 8.1 | | |
| | | $^3J$ = 7.5 | | |
| | | $^4J$ = 1.8 | | |
| **2** | 8.08 (ddd) | 7.80 (ddd) | 7.19 (ddd) | 8.41 (ddd) |
| $CDCl_3$ | $^3J$ = 8.3 | $^3J$ = 8.3 | $^3J$ = 7.4 | $^3J$ = 4.9 |
| | $^4J$ = $^5J$ = 0.9 | $^3J$ = 7.4 | $^3J$ = 4.9 | $^4J$ = 1.8 |
| | | $^4J$ = 1.8 | $^4J$ = 1.0 | $^5J$ = 0.8 |
| **5** | 6.95 (br) | 7.72 (ddd) | 7.35 (dd) | 8.41 (dd) |
| $CD_2Cl_2$ | | $^3J$ = $^3J$ = 7.9 | $^3J$ = 7.4 | $^3J$ = 5.1 |
| | | $^4J$ = 1.6 | $^3J$ = 5.1 | $^4J$ = 1.6 |
| **6** | 7.14 (d) | 7.99 (ddd) | 7.60 (m) | 8.81 (m) |
| $CD_3COCD_3$ | $^3J$ = 8.3 | $^3J$ = $^3J$ = 8.3 | | |
| | | $^4J$ = 1.7 | | |
| **7** | 7.89 (d) | 8.08 (ddd) | 7.35 (ddd) | 8.28 (ddd) |
| $CD_2Cl_2$ | $^3J$ = 8.5 | $^3J$ = 8.5 | $^3J$ = 7.4 | $^3J$ = 5.1 |
| | | $^3J$ = 7.4 | $^3J$ = 5.1 | $^4J$ = 1.7 |
| | | $^4J$ = 1.7 | $^4J$ = 0.7 | $^5J$ = 0.9 |

[a] See Scheme 1 for numbering.

of a hypothetical equilibrium between two forms (**a** and **b**), as represented in Scheme 4. These forms should present an asymmetric metal environment produced by a closer approach to one of the two different coordinated nitrogen atoms (N-Tz or N-Pz). In this way, the environment of the $R^2$ substituent at the 5-position should not be appreciably modified when moving from **a** to **b**, therefore it gives rise to well-defined signals. In contrast, the $R^1$ substituent at the 3-position will be strongly affected by this equilibrium; this causes a broadening of its signals. Dynamic experiments were undertaken, but unfortunately they proved to be inconclusive. A similar explanation was provided for a related case in a previous paper.[4]

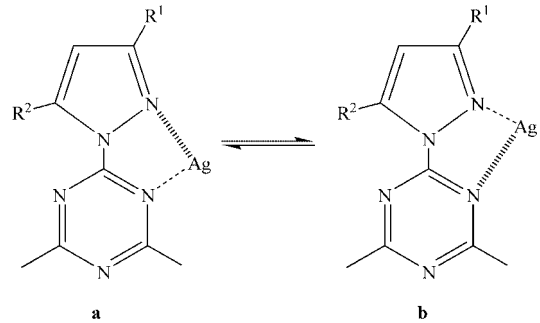


$R^1 = R^2 = C_6H_4OC_4H_9$ **8**
$R^1 = C_6H_4OC_4H_9$; $R^2$ = H **9**

Scheme 4. Hypothetical equilibrium in solution for **8** and **9**.

Table 3 shows the $^{15}$N NMR chemical shifts of ligands **1**–**4** in $CDCl_3$ solution. Those corresponding to complexes **5**–**9** were recorded in solution and/or the solid state, where no fluxional processes would occur. We have already demonstrated that $^{15}$N NMR spectroscopy is the most useful tool for establishing the coordination site, as the increase in the nitrogen shielding on metal complexation reflects the changes in the paramagnetic shielding term.[4,13]

In complexes **5** and **7**, it is clear that both the pyridine N1′ and the pyrazole N2 bind to the metal atom as the

Table 3. $^{15}$N NMR chemical shifts ($\delta$ in ppm).[a] The silver coordination effects on the chemical shifts [$\Delta\delta(^{15}N) = \delta(^{15}N)$complex – $\delta(^{15}N)$ ligand] are given in brackets.

| Compound<br>Solvent | *N*-pyrazole (N-Pz)<br>N1 | <br>N2 | *N*-pyridine (N-Py)<br>N1′ | *N*-triazine (N-Tz)<br>N1′,N3′,N5′ |
|---|---|---|---|---|
| **1** | –166.0 | –85.0 | –84.0 | |
| $CDCl_3$ | | | | |
| **2** | –160.0[b] | –93.0[b] | –105.0[b] | |
| $CDCl_3$ | | | | |
| **3** | –169.0[b,c] | –86.0[b] | | –156.8[b,c] |
| $CDCl_3$ | | | | |
| **4** | –163.0[b,c] | –93.4[b] | | –177.0[c] |
| $CDCl_3$ | | | | |
| **5**[b] | –172.0 | –108.0 (–23) | –118.0 (–34) | |
| $CD_2Cl_2$ | | | | |
| **5** | –167.0 | –97.0 (–12) | –112.0 (–28) | |
| CPMAS | –171.0 | –105.0 (–20) | –119.0 (–35) | |
| **7**[b] | –168.0 | –105.0 (–12) | –129.0 (–24) | |
| $CD_2Cl_2$ | | | | |
| **7** | –163.0 | –114.0 (–21) | –128.0 (–23) | |
| CPMAS | –168.0 | –120.0 (–27) | –130.0 (–25) | |
| **8**[c] | –161.0 | –130.0 (–44) | | –192.0 (–35.2) |
| $CDCl_3$ | | | | |
| **8** | –173.0 | –125.3 (–39.3) | | –195.0 (–38.2) |
| CPMAS | | | | |
| **9** | –165.0 | –123.0 (–29.6) | | –191.0 (–14) |
| CPMAS | | | | |

[a] See Scheme 1 for numbering. [b] ($^1$H-$^{15}$N) gs-HMBC and gs-HMQC spectra. [c] Inverse gated spectra.

  

chemical shifts of their signals move upfield with respect to the free ligands **1** and **2** [$\Delta\delta(^{15}N) = \delta(^{15}N)$complex – $\delta(^{15}N)$ ligand]. In the solid state, the asymmetry of the PzPy units binding the silver cation in the crystal accounts for the two signals observed for each nitrogen. The X-ray structure of **5**, which will described below, supports the above suggestion.

When dealing with the data for **8** and **9** in comparison with those for **3** and **4**, the coordination effects [$\Delta\delta(^{15}N)$] on the triazine N atoms and the pyrazole N2 atom are also negative (Table 3). However, for **5** and **7** the $\Delta\delta$ value for N-Py is higher than that for N-Pz, while the opposite is observed for **8** and **9**. These results agree with a higher crowding of the N-Tz than that of the N-Py.

The $^{15}N$ NMR spectra of **8** in solution show a higher coordination shift for the N2 of the pyrazole than that for the nitrogen atoms of the triazine, which could be related to the greater strength of the Ag–N bond with the pyrazole. This result is in agreement with the proposed asymmetric silver environment for the complexes.

On the other hand, the chemical shift value of N1 of the pyrazole in all complexes is not significantly affected by the metal coordination, as expected due to the absence of its participation in coordination to the metal atom.

The $^{13}C$ NMR spectroscopic data for all complexes in solution and the solid state (Table 4 and Table S1 in the Supporting Information) are also in agreement with the proposed structures. The chemical shifts have been analysed relative to those of the corresponding ligands and the main conclusions are: (a) the chemical shifts of the carbon signals of the 4-butoxyphenyl chains are not shifted upon coordination, (b) a downfield coordination shift of the C4 signal of around +3.5 ppm occurs, (c) the downfield shift of the pyridine carbon signals follows the order C4′ (+2.5 ppm) > C6′ ≈ C5′ (+2.0 ppm) > C3′ (+0.6 ppm), with the C2′ signal showing an upfield shift of 2.5 ppm, (d) an upfield coor-

Table 4. $^{13}C$ NMR chemical shifts ($\delta$ in ppm) and coupling constants ($J$ in Hz) of the pyrazole, pyridine and triazine moieties of compounds **1**–**9**.[a]

| Compound<br>Solvent | C3 | C4 | C5 | C2′ | C3′ | C4′ | C5′ | C6′ |
|---|---|---|---|---|---|---|---|---|
| **1** | 152.4 | 105.5 | 144.9 | 152.7 | 118.9 | 138.0 | 122.1 | 148.5 |
| $CDCl_3$ | $^2J$ = 4.1 | $^1J$ = 174.6 | $^2J$ = 7.6 | $^3J$ = 11.9 | $^1J$ = 166.3 | $^1J$ = 162.6 | $^1J$ = 164.9 | $^1J$ = 180.7 |
| | $^3J$ = 4.1 | | $^3J$ = 3.8 | $^3J$ = 9.3 | | | | $^2J$ = 3.7 |
| | $^3J$ = 4.1 | | $^3J$ = 3.8 | | | | | $^3J$ = 7.4 |
| **2** | 154.0 | 105.3 | 128.5 | 151.9 | 112.7 | 138.9 | 121.3 | 148.2 |
| $CDCl_3$ | $^2J$ = 4.1 | $^1J$ = 175.6 | $^1J$ = 191.7 | $^3J$ = 10.4 | $^1J$ = 169.4 | $^1J$ = 162.5 | $^1J$ = 165.2 | $^1J$ = 180.7 |
| | $^3J$ = 8.3 | $^2J$ = 8.7 | $^2J$ = 9.2 | $^3J$ = 10.4 | $^3J$ = 6.8 | $^3J$ = 6.6 | $^2J$ = 7.3 | $^2J$ = 4.1 |
| | $^3J$ = 4.1 | | | | | | $^3J$ = 7.3 | $^3J$ = 7.3 |
| | $^3J$ = 4.1 | | | | | | | |
| **3** | 154.3 | 109.4 | 147.8 | 164.5 | | 164.5 | | 164.5 |
| $CDCl_3$ | $^2J$ = 3.7 | $^1J$ = 175.5 | $^2J$ = 8.1 | | | | | |
| | $^3J$ = 3.7 | | $^3J$ = 4.0 | | | | | |
| | $^3J$ = 3.7 | | $^3J$ = 4.0 | | | | | |
| **4** | 157.0 | 107.7 | 131.8 | 162.9 | | 162.9 | | 162.9 |
| $CDCl_3$ | $^2J$ = 4.1 | $^1J$ = 177.6 | $^1J$ = 194.9 | | | | | |
| | $^3J$ = 4.1 | | $^2J$ = 9.0 | | | | | |
| | $^3J$ = 4.1 | | | | | | | |
| **5** | 154.0 | 108.6 | 146.8 | 150.1 | 119.2 | 140.1 | 124.0 | 150.5 |
| $CD_2Cl_2$ | $^2J$ = 4.0 | $^1J$ = 178.2 | $^2J$ = 7.8 | $^2J$ = 10.2 | $^1J$ = 170.4 | $^1J$ = 166.3 | $^1J$ = 168.7 | $^1J$ = 184.5 |
| | $^3J$ = 4.0 | | $^3J$ = 4.0 | $^3J$ = 10.2 | $^2J$ = 7.1 | $^2J$ = 6.5 | $^2J$ = 6.8 | $^2J$ = 3.3 |
| | $^3J$ = 4.0 | | | | | $^3J$ = 6.5 | $^3J$ = 6.8 | $^3J$ = 7.6 |
| **5** | 152.6 | 107.8 | 145.1 | 150.1 | 119.5 | 143.5 | 124.5 | 152.0 |
| CPMAS | 153.6 | 109.6 | | | | | | |
| **7** | 154.8 | 108.6 | 131.0 | 149.4 | 113.6 | 141.7 | 123.4 | 149.7 |
| $CD_2Cl_2$ | $^2J$ = 4.0 | $^1J$ = 180.4 | $^1J$ = 191.8 | $^3J$ = 10.1 | $^1J$ = 169.7 | $^1J$ = 166.1 | $^1J$ = 168.7 | $^1J$ = 184.0 |
| | $^3J$ = 8.2 | $^2J$ = 7.4 | $^2J$ = 8.8 | $^3J$ = 10.1 | $^3J$ = 7.0 | | $^2J$ = 6.7 | $^3J$ = 7.2 |
| | $^3J$ = 4.0 | | | | | | $^3J$ = 6.7 | $^2J$ = 4.3 |
| | $^3J$ = 4.0 | | | | | | | |
| **7** | 152.4 | 107.3 | 132.1 | 146.8 | 112.1 | 137.2 | 123.4 | 149.5 |
| CPMAS | | 109.9 | | 148.9 | 114.5 | 138.6 | | 151.0 |
| **8** | 156.2 | 112.6 | 148.0 | 161.7 | | 161.7 | | 161.7 |
| $CDCl_3$ | | $^1J$ = 182.7 | | | | | | |
| **8** | 154.3 | 115.3 | 148.2 | 161.5 | | 161.5 | | 161.5 |
| CPMAS | 155.8 | | | | | | | |
| **9** | 158.7 (br) | 111.1 | 134.4 (br) | 162.1 | | 162.1 | | 162.1 |
| $CD_3COCD_3$ | | $^1J$ = 181.5 | | | | | | |
| | | $^2J$ = 7.2 | | | | | | |
| **9** | 156.0 | 110.0 | 135.3 | 161.5 | | 161.5 | | 161.5 |
| CPMAS | 156.6 | 112.7 | 138.8 | | | | | |

[a] See Scheme 1 for numbering.

  

dination shift of the signals of the three equivalent triazine carbon atoms takes place.

The $^{13}C$ NMR spectra in solution show the equivalence of the pyrazole groups, as well as the inequivalence of their substituents, as already deduced by $^{1}H$ NMR spectroscopy. In the case of $[Ag(Pz^{bp2}Py)_2(OSO_2CF_3)]$ (**5**), the $^{13}C$ CPMAS NMR spectroscopic data indicate that both $Pz^{bp2}Py$ ligands are inequivalent as well as the two 4-butoxyphenyl groups of each ligand, as has also been established by X-ray crystallography. The splitting of the signals observed in all compounds in the solid state can also be attributed to packing effects.

The above results establish a bidentate coordination involving the N-Pz/N-Py in complexes **5** and **7** or N-Pz/N-Tz in **8** and **9**. A new coordinative position around the silver should be occupied by the oxygen atom from the triflate $CF_3SO_3$ groups, giving rise to five-coordinate species containing two PyPz ligands for **5** and **7**, while three-coordination is proposed for **8** and **9**.

In the search for additional structural information, the X-ray structures of **5** and **6** were solved, and the results are described in the following section.

### Crystal and Molecular Structures of 5 and 6

Compounds **5** and **6** crystallised from dichloromethane solutions. Table 5 provides a selected list of bond lengths and angles.

As depicted in Figure 1, the silver centre in **5** is four-coordinate with the nitrogen atoms of two $Pz^{bp2}Py$ ligands in a distorted tetrahedral environment. This is reflected in the dihedral angle formed by the AgN1N3 and AgN4N5 planes of 124.8(2)°. The Ag–N bond lengths fall in the range of 2.28–2.50 Å found for related compounds.[1b,1h,1k,6e,6f,14] The mean Ag–N distance involving the N-Py atoms [2.318(8) Å] is shorter than that of the N-Pz atoms [2.467(8) Å]. The largest distortion from tetrahedral geometry is given by the N–Ag–N bite angle [N1–Ag–N3: 70.9(3)°; N6–Ag–N4: 69.7(3)°] associated with the chelating ligands.

Table 5. Selected bond lengths [Å] and angles [°] for **5** and **6**.

| | | | |
|---|---|---|---|
| | **5** | | |
| Ag–N1 | 2.359(8) | N6–Ag–N1 | 152.5(3) |
| Ag–N3 | 2.385(9) | N6–Ag–N3 | 136.6(3) |
| Ag–N4 | 2.574(8) | N1–Ag–N3 | 70.9(3) |
| Ag–N6 | 2.251(8) | N6–Ag–N4 | 69.7(3) |
| Ag···O5 | 2.704(8) | N1–Ag–N4 | 93.3(3) |
| | | N3–Ag–N4 | 128.2(3) |
| | | N1–Ag···O5 | 94.3(3) |
| | | N3–Ag···O5 | 77.5(3) |
| | | N4–Ag···O5 | 154.3(3) |
| | | N6–Ag···O5 | 93.1(3) |
| | **6** | | |
| Ag–N1 | 2.584(6) | N3–Ag–O3 | 142.4(2) |
| Ag–N3 | 2.307(6) | N3–Ag–N1 | 69.4(2) |
| Ag–O3 | 2.325(6) | O3–Ag–N1 | 103.4(2) |
| Ag–C25[a] | 2.670(7) | N3–Ag–C25C26[b] | 116.3(2) |
| Ag–C26[a] | 2.706(7) | O3–Ag–C25C26[b] | 101.5(3) |
| Ag–C25C26[b] | 2.598(1) | N1–Ag–C25C26[b] | 104.9(2) |

[a] $-x + 1, -y + 1, -z + 1$. [b] C25C26 means the centroid of the C25–C26 bond.

The $C_6H_4$ group at the 3-position in one molecule of **5** is almost parallel to the $C_6H_4$ group at the 5-position of the other molecule [dihedral angle of 4.2(3)°], and the remaining aryl rings are orthogonal between them [86.7(2)°] with the butoxy chains in an opposite and almost symmetrical disposition. The four chains produce a crowding in one corner of the metal environment. As a consequence, the silver centre has a deprotected position that allows the approach of an oxygen atom of the triflate group. The Ag···O5 distance of 2.704(8) Å is smaller than the sum of the van der Waals radii of 2.84 Å.[14b] Similar values have been attributed to metal–oxygen bonds.[1h,1m,9] Therefore, the distance observed for **5** can be considered a "strong" coordinative interaction, giving rise to a distorted trigonal bipyramidal geometry around the metal atom.

Because of the usually found three-coordination around the silver centre, we thought that the coordination of the triflate group could be assessed by using a ratio of $Pz^{bp2}Py$ ligand/$Ag(OSO_2CF_3)$ = 1.

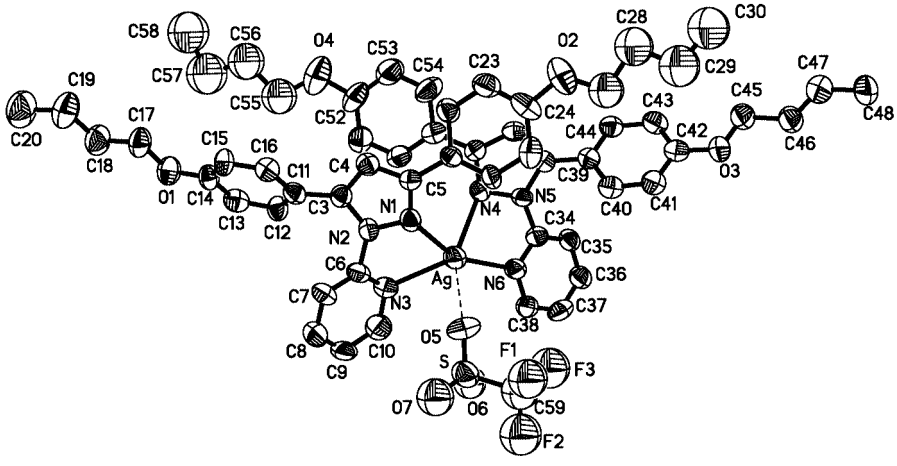


Figure 1. ORTEP plot of **5** with ellipsoids at 40% probability, showing the $Pz^{bp2}Py$ coordination and the Ag···O intermolecular bonds. Hydrogen atoms and the labelling of some atoms have been omitted for clarity.

  

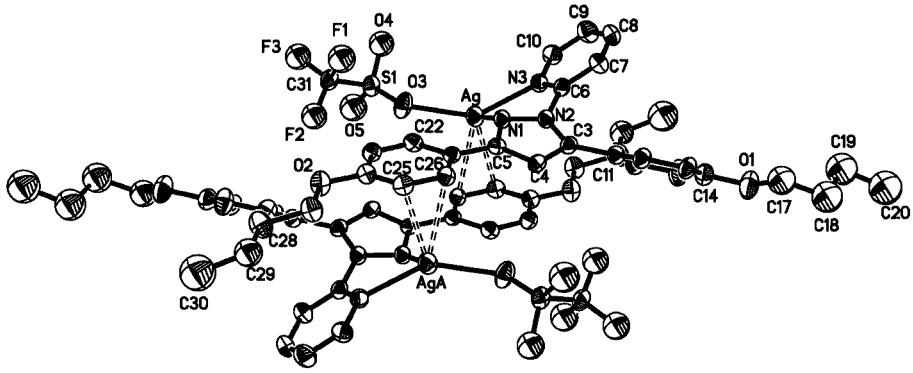


Figure 2. ORTEP plot of **6** with ellipsoids at 35% probability level, showing the dimeric unit formed by Ag···arene interactions. Hydrogen atoms and the labelling of some atoms have been omitted for clarity.

The molecular structure of **6** is shown in Figure 2 and corresponds to a dimeric entity produced by Ag···π(aryl ring) interactions between two molecules that are symmetrically related by an inversion centre. The coordination geometry around each silver atom in **6** is quite different from that in **5**. Thus, the metal atom in **6** adopts the usual three-coordination with the silver cation being trigonally coordinated by the two nitrogen atoms of the bidentate $Pz^{bp2}Py$ ligand and an oxygen atom from the triflate anion. The Ag–N1 and Ag–N5 distances of 2.584(6) and 2.307(6) Å, respectively, are almost equivalent to those found in **5**. The metal atom deviates 0.741(1) Å from the plane defined by the three coordinated atoms (N1, N3, O), this deviation being produced by the proximity of an aryl group from the second molecule, to which the silver atom is also coordinated by an Ag···π bond,[15] thus generating a distorted tetrahedral environment. The short Ag–C distances [mean value of 2.668(7) Å] are in the range found in other compounds containing $\eta^2$-Ag···π arene interactions (2.40–2.75 Å).[9,16] The contacts of the silver atom with the other aromatic carbon atom are greater than 3 Å [the shortest is Ag–C24 ($-x + 1$, $-y + 1$, $-z + 1$) with 3.22(3) Å], consisting of an asymmetric coordination of the silver atom with the two carbon atoms of the benzene ring. The separation of each silver atom from the mean plane of its coordinated aryl group of 2.567(5) Å lies in the range inherent to the bonding of an arene ligand.[16a] In addition, the positional parameters $\beta$ and $\Delta$ (where $\Delta$ and $\beta$ measure the deviation from the centroid axis;[16a] see Scheme 5) of the silver centre of 30.9° and 1.54 Å, respectively, are in agreement with the range of other structures showing an $\eta^2$-coordination of the arene.[16a] All the above arguments allow us unequivocally to establish the presence of a dimerisation through an $\eta^2$-Ag···π arene bond.

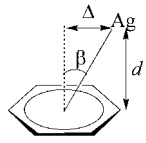


Scheme 5. $\Delta$ and $\beta$ parameters for Ag···arene interactions.[16a]

In the crystal structures of **5** and **6** shown in Figures 3–6, the triflate anion intervenes in the organisation around the $[Ag(Pz^{bp2}Py)_2O]$ and $[Ag(Pz^{bp2}Py)O]$ units, either coordinating or forming a covalent bond with the metal atom in **5** and **6**, respectively. Such an anion is also employed to expand the supramolecular environment with one of the remaining oxygen atoms interacting with the silver centre or carbon atoms of neighbouring units. Thus, the coordination of the anion in **6**, or strong interaction in **5**, can be considered as the first stage of the supramolecular organi-

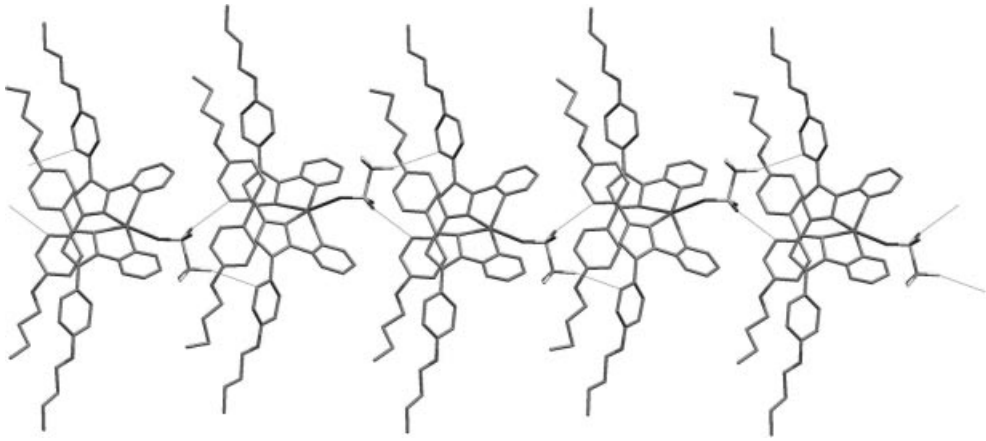

Figure 3. View of the strand along the *b* axis in **5**, showing the Ag···O, C–H···O and C–H···F contacts.

  

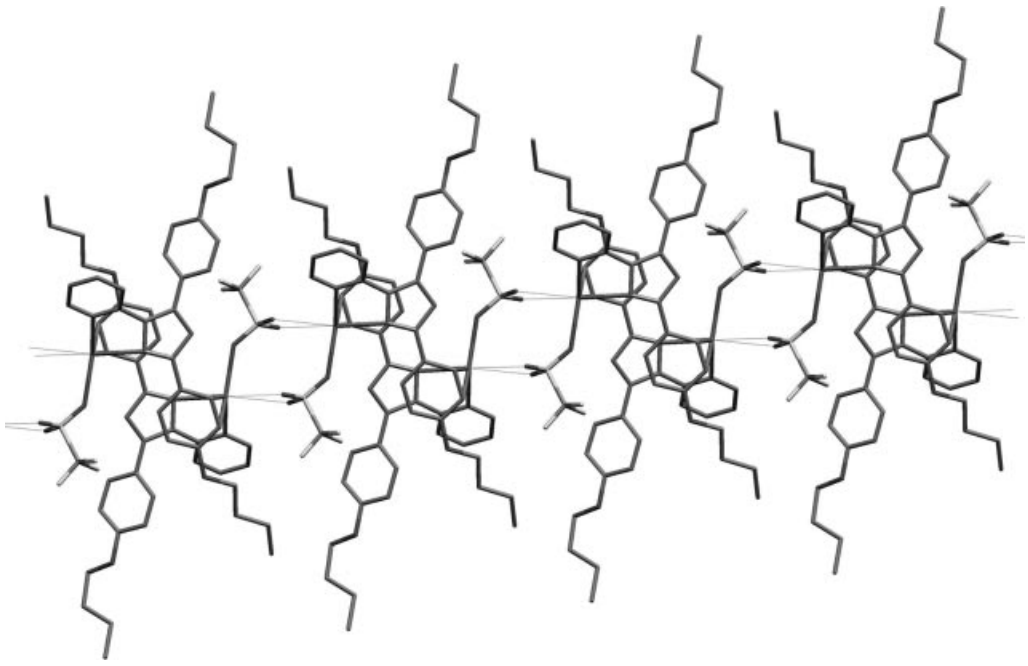

Figure 4. View of the double strand along the *b* axis in **6**, showing the Ag···O contacts between dimers.

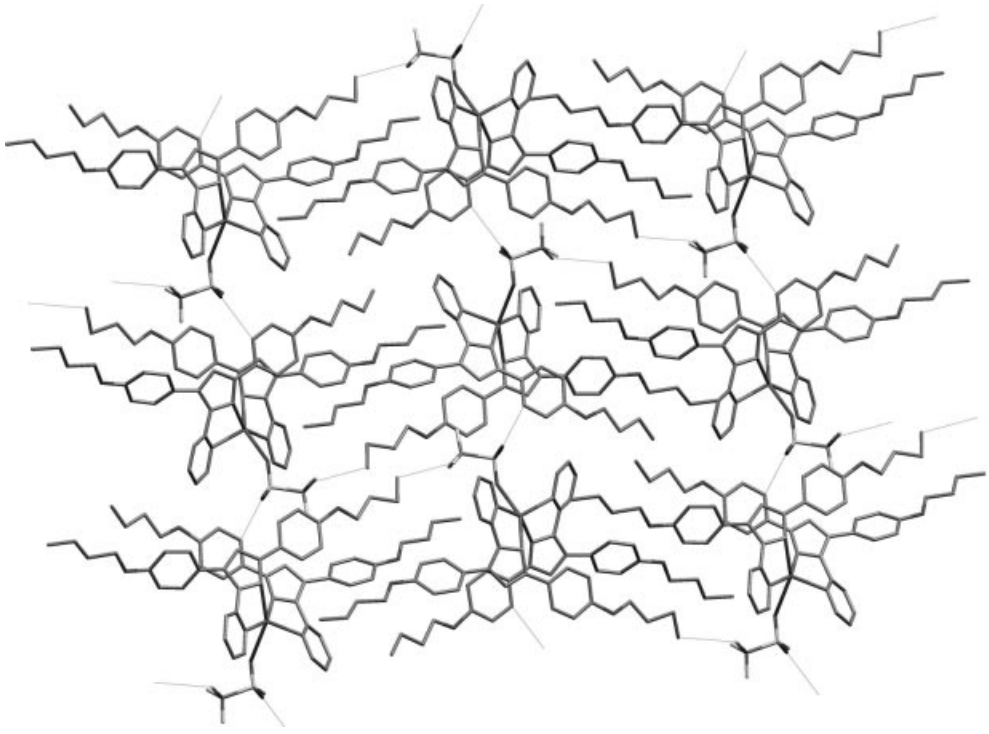

Figure 5. View of a layer parallel to the (101) plane of the 2D network of **5**.

sation, while the next one is consistent with the assembly of $[Ag(Pz^{bp2}Py)_2O]$ and $[Ag(Pz^{bp2}Py)O]$ units, which can be described as follows:

i) The oxygen atoms of the triflate, which are not involved in a direct bond or interaction with the silver atom, are bonded to a pair of adjacent molecules by Ag···O or C–H···O/F interactions, thus generating strands. In **5**, the strands are defined along the *b* axis by the C22···O7 [$-x$ + ½ + 1, $y$ – ½, $-z$ + ½: 3.24(2) Å] and C16···F2 [$-x$ + ½ + 1, $y$ – ½, $-z$ + ½: 3.04(2) Å] interactions (Figure 3). In **6**, the overall arrangement consists of a double strand along the *b* axis in which two triflate anions act as bridging groups of each neighbouring dimer [Ag1···O5 ($-x$ + 1, $-y$ + 2, $-z$ + 1): 2.84(1) Å; Ag1···O4 ($-x$ + 1, $-y$ + 2, $-z$ + 1): 3.32(1) Å; see Figure 4). In addition to related C–H···O interactions [C10···O5 ($-x$ + 1, $-y$ + 2, $-z$ + 1): 3.24(2) Å;

  

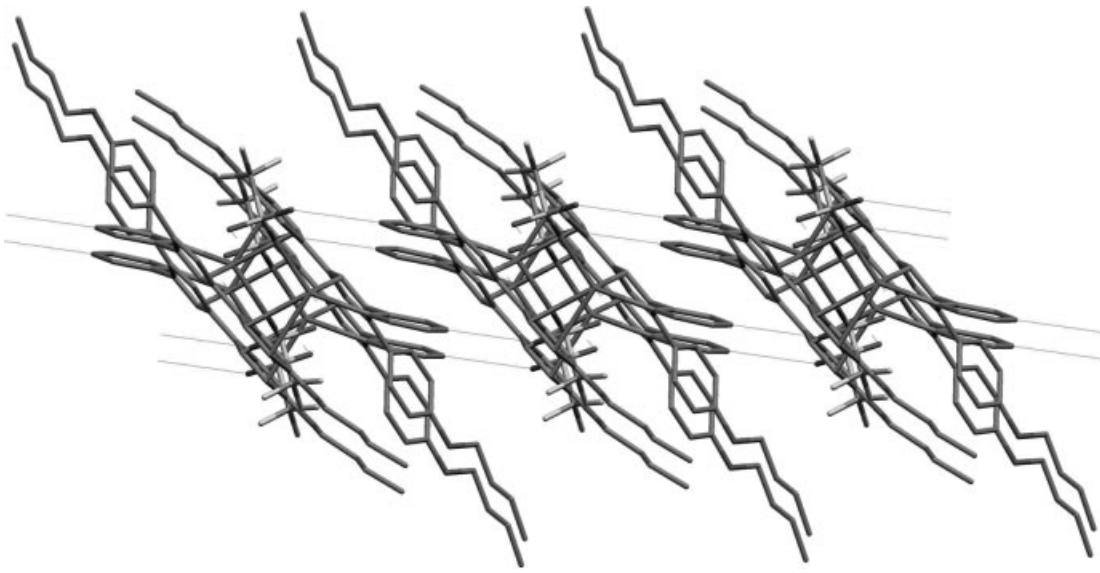

Figure 6. View of a layer parallel to the (001) plane of the 2D network of **6**.

C25···O4 ($x$, $y$ – 1, $z$): 3.18(2) Å], the strands are mainly determined by a direct Ag···O bond. The triflate tecton in both **5** and **6** is responsible for the 1D arrangement.
ii) New non-conventional hydrogen-bonding interactions involving the $CF_3$ groups of the triflate group in **5** or bifurcated C–H···O interactions in **6** extend the supramolecular arrangements into a 2D network. Thus, the C–H···F interactions between the chains in **5** [C58···F3 ($x$ + ½, $-y$ + ½ + 1, $z$ – ½): 3.25(3) Å], where the F atoms proceed from alternating and symmetrically disposed bridging triflate groups along the $c$ axis of the chain, give rise to layers which lie parallel to the (101) plane (Figure 5). In **6**, the same oxygen atom implicated in the strand interacts with the pyridine group of an adjacent strand [C8···O4 ($-x$, $y$ + 2, $-z$ + 1): 3.31(1) Å], thereby extending these interactions through the (001) plane (Figure 6).

## Concluding Remarks

Silver(I) coordination complexes containing $Pz^{bp2}Py$ (**1**), $Pz^{bp}Py$ (**2**), $TPz^{bp2}Tz$ (**3**) and $TPz^{bp}Tz$ (**4**) polydentate ligands have been obtained. An *N*,*N*′-bidentate coordination has been established in $[Ag(Pz^{bp2}Py)_2(OSO_2CF_3)]$ (**5**) and $[Ag(Pz^{bp}Py)_2(OSO_2CF_3)]$ (**7**), which involves the N-Pz/N-Py sites, and implicates the N-Pz/N-Tz ones in $[Ag_3(TPz^{bp2}Tz)(OSO_2CF_3)_3]$ (**8**) and $[Ag_3(TPz^{bp}Tz)(OSO_2CF_3)_3]$ (**9**). A new coordinative position is occupied by the oxygen atom from the triflate groups, giving rise to five-coordinate species containing two PzPy ligands for **5** and **7**, while three-coordination is proposed for **8** and **9**.

The compound $[Ag_2(Pz^{bp2}Py)_2(OSO_2CF_3)_2]$ (**6**), which contains Ag/$Pz^{bp2}Py$ in a 1:1 stoichiometric ratio, exhibits the expected metal environment determined by the *N*,*N*′-bidentate $Pz^{bp2}Py$ ligand and the oxygen atom of the triflate group. However, in this case, this environment is expanded through an M–π olefinic bond to give rise to dimeric units.

From the comparative study of the structures of **5** and **6**, several features can be established as determining factors of the supramolecular arrays: i) The structural role of the triflate anion takes place by coordination or strong interaction of the silver centre to an oxygen atom (Ag···O); ii) the coordination of the anion to the $[Ag(Pz^{bp2}Py)_2]^+$ units in **5** is less favoured than in **6** due to the crowding around the metal centre, which prevents the additional Ag···π interaction that is responsible for the dimer in **6**; iii) double or single strands are built on the basis of hydrogen-bonding interactions.

## Experimental Section

**Materials and Instrumentation:** All commercial reagents were used as supplied. 3-(4-Butoxyphenyl)pyrazole ($HPz^{bp}$), 2-[3,5-bis(4-butoxyphenyl)pyrazol-1-yl]pyridine ($Pz^{bp2}Py$, **1**) and 2,4,6-tris[3,5-bis(4-butoxyphenyl)pyrazol-1-yl]-1,3,5-triazine ($TPz^{bp2}Tz$, **3**) were prepared according to the literature.[4,7,17] Commercial solvents were dried prior to use. Elemental analyses for C, H, N, S were carried out by the Microanalytical Service of the Complutense University. IR spectra were recorded with an FTIR Nicolet Magna-550 spectrophotometer with samples as KBr pellets in the 4000–400 $cm^{-1}$ region. The exact mass of **4** was determined by high resolution mass spectrometry at 70 eV using the electron impact mode with a VG AutoSpec spectrometer.

**NMR Parameters:** Spectra were recorded at 298 K with a Bruker DRX 400 spectrometer (400.13 MHz for $^1H$; 100.62 MHz for $^{13}C$; 40.56 MHz for $^{15}N$ NMR), except for compound **6**, where only the $^1H$ NMR spectrum was registered with a Bruker AC 200 spectrometer. Chemical shifts ($\delta$ in ppm) are given relative to internal solvents [$CDCl_3$ ($\delta$ = 7.26 ppm), $CD_2Cl_2$ ($\delta$ = 5.32 ppm) and $(CD_3)_2CO$ ($\delta$ = 2.05 ppm) for $^1H$ NMR; $^{13}CDCl_3$ ($\delta$ = 77.0 ppm), $CD_2Cl_2$ ($\delta$ = 54.0 ppm) and $(CD_3)_2CO$ ($\delta$ = 29.9 and 206.7 ppm) for $^{13}C$ NMR; external nitromethane ($\delta$ = 0.0 ppm) for $^{15}N$ NMR]. Coupling constants ($J$ in Hz) are accurate to ±0.2 Hz for $^1H$ and $^{13}C$. $^2D$ inverse proton detected heteronuclear shift correlation spectra, $^1H$-$^{13}C$ gs-HMQC, $^1H$-$^{13}C$ gs-HMBC, $^1H$-$^{15}N$ gs-HMBC and $^1H$-

  

$^{15}$N gs-HMQC were recorded with the standard pulse sequences.[18] Solid-state $^{13}$C (100.73 MHz) and $^{15}$N (40.60 MHz) CPMAS NMR spectra were recorded with a Bruker WB-400 spectrometer at 300 K using a 4-mm DVT probehead. Samples were carefully packed in 4-mm diameter cylindrical zirconia rotors with Kel-F end-caps. Operating conditions involved 3.2-μs, 90° $^{1}$H pulses and a decoupling field strength of 78.1 kHz with the TPPM sequence. $^{13}$C NMR spectra were originally referenced to a glycine sample and then the chemical shifts were recalculated relative to $SiMe_4$ [for the carbonyl atom: $\delta$(glycine) = 176.1 ppm], and $^{15}$N spectra to $^{15}NH_4Cl$ and then converted to the nitromethane scale using the relationship $\delta(^{15}N)MeNO_2 = \delta(^{15}N)NH_4Cl - 338.1$ ppm. The typical acquisition parameters for $^{13}$C CPMAS were: spectral width: 40 kHz; recycle delay: 5 s; acquisition time: 30 ms; contact time: 2 ms; accumulation number: 900–2200; spin rate: 12 kHz. In order to distinguish protonated and unprotonated carbon atoms, the NQS (non-quaternary suppression) experiment by conventional cross-polarisation was recorded; before the acquisition, the decoupler was switched off for a very short time of 25 μs.[18] Those for $^{15}$N CPMAS were: spectral width: 40 kHz; recycle delay: 5 s; acquisition time: 35 ms; contact time: 6 ms; accumulation number: 80000–115000; and spin rate: 6 kHz.

**Synthesis of 2-[3-(4-Butoxyphenyl)pyrazol-1-yl]pyridine ($Pz^{bp}Py$, 2):** A solution of 4-butoxyacetophenone (1.81 g, 9.42 mmol) in ethyl formate (1.16 mL, 14.13 mmol) and toluene (15 mL) was added to a slurry of anhydrous sodium methoxide (0.51 g, 9.42 mmol) in toluene (50 mL). A clear solution was obtained, which became a slurry after 5 min. The solid was isolated by filtration after 2 h at room temperature and washed with hexane. The solid obtained (0.36 g, 1.48 mmol) was dissolved in 96% ethanol (10 mL), and then treated with hydrochloric acid (ca. 2.5 mL, spec. grav. 1.18). 2-Hydrazinopyridine (0.65 g, 5.92 mmol) dissolved in the minimum amount of 96% ethanol was added to this solution. The mixture was refluxed for 3 h, and then the solvent was evaporated to about half the original volume and the resulting solution kept in a refrigerator at 4 °C. Pale-yellow needles were obtained after 2 d, which were filtered off and washed with hexane. Yield: 0.30 g (69%). M.p. 79 °C. $C_{18}H_{19}N_3O$ (293.37): calcd. C 73.70, H 6.53, N 14.32; found C 73.61, H 6.45, N 14.25. IR (KBr): $\tilde{\nu}$ = 1616 and 1580 cm$^{-1}$ $\nu$(C=N).

**Synthesis of 2,4,6-Tris[3-(4-butoxyphenyl)pyrazol-1-yl]-1,3,5-triazine ($TPz^{bp}Tz$, 4):** NaH (95%, 63.9 mg, 2.53 mmol) was added to a solution of $HPz^{bp}$ (438.5 mg, 2.03 mmol) in freshly distilled dry THF (30 mL) under argon. After 1.5 h at 90 °C, the solution was allowed to cool, and 2,4,6-trichlorotriazine (cyanuric chloride, 126.1 mg, 0.677 mmol) was added. The solution was heated at 90 °C for 11.5 h and at 60 °C for 15 h. The solvent was evaporated and the residue chromatographed on 60-$F_{254}$ silica gel with chloroform/acetonitrile (92:8) as eluent. $R_f$ = 0.35. Yield: 122 mg (25%). M.p. 197–199 °C. Exact mass calcd. for $C_{42}H_{45}N_9O_3$: 723.3645; found 723.5. IR (KBr): $\tilde{\nu}$ = 1612 cm$^{-1}$ $\nu$(C=N).

**Synthesis of $[Ag(Pz^{bp2}Py)_2(OSO_2CF_3)]$ (5):** $Ag(OSO_2CF_3)$ (45 mg, 0.17 mmol) was added under nitrogen to a solution of $Pz^{bp2}Py$ (**1**; 153 mg, 0.34 mmol) in dry THF (40 mL). After 24 h of stirring, the solution was filtered through a plug of Celite. Then, the solvent was removed in vacuo and 10 mL of dichloromethane was added. The solution was again filtered through a plug of Celite and concentrated. A colourless solid was isolated after addition of hexane at 4 °C. The product was crystallised from a solution of dichloromethane and hexane at 4 °C. Yield: 111 mg (38%). $C_{57}H_{62}AgF_3N_6O_7S$ (1140.1): calcd. C 60.05, H 5.48, N 7.37, S 2.81; found C 59.65, H 5.34, N 7.34, S 2.78. IR (KBr): $\tilde{\nu}$ = 1612 and 1573 cm$^{-1}$ $\nu$(C=N), 1273 $\nu_{as}(SO_3)$, 1028 $\nu_s(SO_3)$.

**Synthesis of $[Ag_2(Pz^{bp2}Py)_2(OSO_2CF_3)_2]$ (6):** This compound was prepared in a similar way to **5**, from $Ag(OSO_2CF_3)$ (35 mg, 0.14 mmol) and $Pz^{bp2}Py$ (**1**; 60 mg, 0.14 mmol). The product was crystallised from a solution of dichloromethane at 4 °C. Yield: 38 mg (40%). $C_{58}H_{62}Ag_2F_6N_6O_{10}S_2$ (1397.0): calcd. C 49.87, H 4.47, N 6.02, S 4.59; found C 49.82, H 4.57, N 5.93, S 4.56. IR (KBr): $\tilde{\nu}$ = 1605 and 1572 cm$^{-1}$ $\nu$(C=N), 1288 $\nu_{as}(SO_3)$, 1027 $\nu_s(SO_3)$.

**Synthesis of $[Ag(Pz^{bp}Py)_2(OSO_2CF_3)]$ (7):** The compound was prepared in a similar way to **5**, from $Ag(OSO_2CF_3)$ (87 mg, 0.34 mmol) and $Pz^{bp}Py$ (**2**; 200 mg, 0.68 mmol). The product was recrystallised from dichloromethane/hexane at 4 °C. Yield: 109 mg (38%). $C_{37}H_{38}AgF_3N_6O_5S$ (843.7): calcd. C 52.68, H 4.54, N 9.96, S 3.80; found C 52.49, H 4.47, N 9.95, S 3.81. IR (KBr): $\tilde{\nu}$ = 1608 and 1578 cm$^{-1}$ $\nu$(C=N), 1249 $\nu_{as}(SO_3)$, 1031 $\nu_s(SO_3)$.

**Synthesis of $[Ag_3(TPz^{bp2}Tz)(OSO_2CF_3)_3]$ (8):** $Ag(OSO_2CF_3)$ (33.7 mg, 0.13 mmol) was added to a solution of $TPz^{bp2}Tz$ (50.6 mg, 0.04 mmol) in 30 mL of dry THF. After 24 h of stirring, the solution was filtered through a plug of Celite. The solvent was then evaporated to about 5 mL, and pentane (10 mL) was added. The yellow solid formed was filtered off, washed with small portions of pentane and dried in vacuo. Yield: 40 mg (48%). $C_{75}H_{81}Ag_3F_9N_9O_{15}S_3$ (1939.3): calcd. C 46.45, H 4.21, N 6.50; found C 46.49, H 4.36, N 6.49. IR (KBr): $\tilde{\nu}$ = 1610 cm$^{-1}$ $\nu$(C=N), 1253 $\nu_{as}(SO_3)$, 1027 $\nu_s(SO_3)$.

**Synthesis of $[Ag_3(TPz^{bp}Tz)(OSO_2CF_3)_3]$ (9):** The compound was prepared as described for **8**, from $TPz^{bp}Tz$ (31.4 mg, 0.04 mmol) and $Ag(OSO_2CF_3)$ (33.3 mg, 0.13 mmol). Yield: 41.2 mg (63%). $C_{45}H_{45}Ag_3F_9N_9O_{12}S_3$ (1494.7): calcd. C 36.16, H 3.03, N 8.43; found C 36.34, H 3.41, N 8.38. IR (KBr): $\tilde{\nu}$ = 1610 cm$^{-1}$ $\nu$(C=N), 1253 $\nu_{as}(SO_3)$, 1027 $\nu_s(SO_3)$.

**X-ray Structure Determinations:** Colourless thin plate or prismatic single crystals of $[Ag(Pz^{bp2}Py)_2(OSO_2CF_3)]$ (**5**) and $[Ag_2(Pz^{bp2}Py)_2(OSO_2CF_3)_2]$ (**6**), respectively, were grown from dichloromethane solutions. Data collection was carried out at room temperature with a Bruker Smart CCD diffractometer using graphite-monochromated Mo-$K_\alpha$ radiation ($\lambda$ = 0.71073 Å) operating at 50 kV and 20 mA. In all cases, data were collected over a hemisphere of the reciprocal space by combination of three exposure sets. Each exposure covered 0.3° in $\omega$. The cell parameters were determined and refined by a least-squares fit of all reflections collected. The first 50 frames were recollected at the end of the data collection to monitor crystal decay; no appreciable decay was observed. A summary of the fundamental crystal and refinement data is given in Table 6. The structures were solved by direct methods and refined by full-matrix least squares on $F^2$.[19] Anisotropic parameters were used in the last cycles of refinement for all non-hydrogen atoms, with some exceptions. Thus, some carbon atoms of the butoxy chains, the fluorine and only two oxygen atoms of the triflate group were refined isotropically. The third oxygen atom of the triflate group, which interacts with the silver atom, was refined anisotropically. Some of these atoms were refined with geometrical restraints and variable common carbon–carbon and carbon–oxygen distances. Hydrogen atoms were included in calculated positions, and refined as riding on their respective carbon atoms with thermal parameters related to the bonded atoms. Hydrogen atoms were analysed with SHELXS-97 and PARST97.[20] The largest residual peaks in the final difference map were 1.173 and 1.266 e Å$^{-3}$ for **5** and **6**, respectively, in the vicinity of the fluorine atoms. CCDC-266326 (**5**) and -266327 (**6**) contain the supplementary crystallographic data for this paper. These data can be obtained free of

  

Table 6. Crystal and refinement data for **5** and **6**.

| | **5** | **6** |
|---|---|---|
| Empirical formula | $C_{57}H_{62}AgF_3N_6O_7S$ | $C_{58}H_{62}Ag_2F_6N_6O_{10}S_2$ |
| Formula mass | 1140.06 | 1397.03 |
| Crystal system | monoclinic | triclinic |
| Space group | $P2_1/n$ | $P\bar{1}$ |
| $a$ [Å] | 9.4058(6) | 10.602(1) |
| $b$ [Å] | 22.149(1) | 10.912(1) |
| $c$ [Å] | 26.704(2) | 14.735(1) |
| $\alpha$ [°] | 90 | 72.466(2) |
| $\beta$ [°] | 98.577(1) | 73.340(2) |
| $\gamma$ [°] | 90 | 72.473(2) |
| $V$ [Å$^3$] | 5508.4(6) | 1513.6(4) |
| $Z$ | 4 | 1 |
| $F$(000) | 2368 | 1456 |
| $D_{calcd.}$ [g cm$^{-3}$] | 1.375 | 1.537 |
| $T$ [K] | 296(2) | 296(2) |
| $\mu$(Mo-$K_\alpha$) [mm$^{-1}$] | 0.471 | 0.796 |
| Crystal size [mm] | 0.45 × 0.25 × 0.05 | 0.28 × 0.17 × 0.05 |
| Scan technique | φ and ω | φ and ω |
| Data collected | –11,–24,–27 to 11,26,31 | –12,–12,–17 to 6,10,17 |
| $\theta$ [°] | 1.20–25.00 | 1.48–25.00 |
| Refls. collected | 28738 | 7954 |
| Refls. indep. | 9664 ($R_{int}$ = 0.120) | 5269 ($R_{int}$ = 0.038) |
| Data/restraints/parameters | 9664/13/592 | 5269/10/305 |
| Refls. observed [$I > 2\sigma(I)$] | 3211 | 2965 |
| GOF ($F^2$) | 0.899 | 0.973 |
| $R(F)$[a] | 0.089 | 0.069 |
| $wR(F^2)$ (all data)[b] | 0.328 | 0.222 |
| Largest residual peak [e Å$^{-3}$] | 1.173 | 1.266 |

[a] $\Sigma(|F_o| - |F_c|)/\Sigma|F_o|$. [b] $\{\Sigma[w(F_o^2 - F_c^2)^2]/\Sigma[w(F_o^2)^2]\}^{1/2}$.

charge from The Cambridge Crystallographic Data Centre via www.ccdc.cam.ac.uk/data_request/cif.

## Acknowledgments

Financial support from the Dirección General de Investigación/ Ministerio de Ciencia y Tecnología is gratefully acknowledged (projects BQU2003-07343 and BQU2003-00976).

[1] a) P. M. Hagrman, D. Hagrman, J. Zubieta, *Angew. Chem.* **1999**, *111*, 2798–2848; *Angew. Chem. Int. Ed.* **1999**, *38*, 2638–2684; b) L. Carlucci, G. Ciani, D. M. Prosperio, A. Sironi, *J. Am. Chem. Soc.* **1995**, *117*, 4562–4569; c) A. J. Blake, N. R. Champness, P. Hubberstey, W.-S. Li, M. A. Withersby, M. Schröder, *Coord. Chem. Rev.* **1999**, *183*, 117–138; d) O. M. Yaghi, H. Li, *J. Am. Chem. Soc.* **1996**, *118*, 295–296; e) A. J. Blake, N. R. Champness, M. Crew, S. Parsons, *New J. Chem.* **1999**, *23*, 13–15; f) F. Robinson, M. J. Zaworotko, *J. Chem. Soc., Chem. Commun.* **1995**, 2413–2414; g) C. V. K. Sharma, S. T. Griffin, R. D. Rogers, *Chem. Commun.* **1998**, 215–216; h) D. Venkataraman, S. Lee, J. S. Moore, P. Zhang, K. A. Hirsch, G. B. Gardner, A. C. Covey, C. L. Prentice, *Chem. Mater.* **1996**, *8*, 2030–2040; i) R. G. Vranka, E. L. Amma, *Inorg. Chem.* **1966**, *5*, 1020–1025; j) L. Carlucci, G. Ciani, D. M. Proserpio, A. Sironi, *J. Chem. Soc., Chem. Commun.* **1994**, 2755–2756; k) M. Munakata, M. Wen, Y. Suenaga, T. Kuroda-Sowa, M. Maekawa, M. Anahata, *Polyhedron* **2001**, *20*, 2037–2043; l) W.-H. Bi, D.-F. Sun, R. Cao, M.-C. Hong, *Acta Crystallogr., Sect. E* **2002**, *58*, m324–m325; m) M.-L. Tong, X.-M. Chen, S. W. Ng, *Inorg. Chem. Commun.* **2000**, *3*, 436–441; n) A. Jouaiti, M. W. Hosseini, N. Kyritsakas, *Eur. J. Inorg. Chem.* **2003**, 57–61.

[2] a) T. C. W. Mak, *Inorg. Chim. Acta* **1984**, *84*, 19–23; b) B.-L. Fei, W.-Y. Sun, T. Okamura, W.-X. Tang, N. Ueyama, *New J. Chem.* **2001**, *25*, 210–212; c) A. Bacchi, E. Bossetti, M. Carcelli, P. Pelagatti, D. Rogolino, *Eur. J. Inorg. Chem.* **2004**, 1985–1991; d) Q.-Y. Zhu, J. Dai, D.-X. Jia, L.-H. Cao, H.-H. Lin, *Polyhedron* **2004**, *23*, 2259–2264; e) D. L. Reger, J. R. Gardinier, R. F. Semeniuc, M. D. Smith, *Dalton Trans.* **2003**, 1712–1718; f) D. L. Reger, J. R. Gardinier, M. D. Smith, *Inorg. Chem.* **2004**, *43*, 3825–3832; g) D. Venkataraman, G. B. Gardner, S. Lee, J. S. Moore, *J. Am. Chem. Soc.* **1995**, *117*, 11600–11601; h) K. A. Hirsch, D. Venkataraman, S. R. Wilson, J. S. Moore, S. Lee, *J. Chem. Soc., Chem. Commun.* **1995**, 2199–2200; i) C. L. Schauer, E. Matwey, F. W. Fowler, J. W. Lauher, *J. Am. Chem. Soc.* **1997**, *119*, 10245–10246; j) M. Bertelli, L. Carlucci, G. Ciani, D. M. Proserpio, A. Sironi, *J. Mater. Chem.* **1997**, *7*, 1271–1276; k) S. R. Batten, R. Robson, *Angew. Chem.* **1998**, *110*, 1558–1595; *Angew. Chem. Int. Ed.* **1998**, *37*, 1460–1494; l) R. Wang, M.-C. Hong, J. Luo, F. Jiang, L. Han, Z. Lin, R. Cao, *Inorg. Chim. Acta* **2004**, *357*, 103–114.

[3] M. Cano, J. V. Heras, M. L. Gallego, J. Perles, C. Ruiz-Valero, E. Pinilla, M. R. Torres, *Helv. Chim. Acta* **2003**, *86*, 3194–3203.

[4] R. M. Claramunt, P. Cornago, M. Cano, J. V. Heras, M. L. Gallego, E. Pinilla, M. R. Torres, *Eur. J. Inorg. Chem.* **2003**, 2693–2704.

[5] M. L. Gallego, P. Ovejero, M. Cano, J. V. Heras, J. A. Campo, E. Pinilla, M. R. Torres, *Eur. J. Inorg. Chem.* **2004**, 3089–3098.

[6] a) M. A. Withersby, A. J. Blake, N. R. Champness, P. Hubberstey, W.-S. Li, M. Schröder, *Angew. Chem.* **1997**, *109*, 2421–2423; *Angew. Chem. Int. Ed. Engl.* **1997**, *36*, 2327–2329; b) M. J. Hannon, C. L. Painting, W. Errington, *Chem. Commun.* **1997**, 1805–1806; c) A. J. Blake, N. R. Champness, S. S. M. Chung, W.-S. Li, M. Schröder, *Chem. Commun.* **1997**, 1675–1676; d) B. F. Hoskins, R. Robson, D. A. Slizys, *J. Am. Chem. Soc.* **1997**, *119*, 2952–2953; e) L. Carlucci, G. Ciani, D. M. Proserpio, A. Sironi, *Inorg. Chem.* **1995**, *34*, 5698–5700; f) L. Carlucci, G. Ciani, D. M. Proserpio, A. Sironi, *Angew. Chem.* **1995**, *107*, 2037–2040; *Angew. Chem. Int. Ed. Engl.* **1995**, *34*, 1895–1898; g) L. Carlucci, G. Ciani, D. W. v. Gudenberg, D. M. Proserpio, *Inorg. Chem.* **1997**, *36*, 3812–3813.

  

[7] J. A. Campo, M. Cano, J. V. Heras, M. C. Lagunas, J. Perles, E. Pinilla, M. R. Torres, *Helv. Chim. Acta* **2002**, *85*, 1079–1095.
[8] a) M. Burgos, O. Crespo, M. C. Gimeno, P. G. Jones, A. Laguna, *Eur. J. Inorg. Chem.* **2003**, 2170–2174; b) I. Boldog, E. B. Rusanov, A. N. Chernega, J. Sieler, K. V. Domasevith, *Polyhedron* **2001**, *20*, 887–897.
[9] M. Munakata, L. P. Wu, T. Kuroda-Sowa, M. Maekawa, Y. Suenaga, G. L. Ning, T. Kojima, *J. Am. Chem. Soc.* **1998**, *120*, 8610–8618.
[10] M. Munakata, M. Wen, Y. Suenaga, T. Kuroda-Sowa, M. Maekawa, M. Anahata, *Polyhedron* **2001**, *20*, 2321–2327.
[11] G. A. Lawrance, *Chem. Rev.* **1986**, *86*, 17–33.
[12] D. L. Reger, J. R. Gardinier, T. C. Grattan, M. R. Smith, M. D. Smith, *New J. Chem.* **2003**, *27*, 1670–1677.
[13] P. Cornago, R. M. Claramunt, M. Cano, J. V. Heras, M. L. Gallego, *ARKIVOC* **2005**, (ix), 21–29.
[14] a) D. L. Reger, R. F. Semeniuc, M. D. Smith, *Inorg. Chem. Commun.* **2002**, *5*, 278–282; b) C.-J. Lin, W.-S. Hwang, M. Y. Chiang, *Polyhedron* **2001**, *20*, 3275–3280.
[15] a) M. Munakata, L. P. Wu, T. Kuroda-Sowa, *Adv. Inorg. Chem.* **1999**, *46*, 173–303; b) M. Munakata, L. P. Wu, G. L. Ning, *Coord. Chem. Rev.* **2000**, *198*, 171–203.
[16] a) S. V. Lindeman, R. Rathore, J. K. Kochi, *Inorg. Chem.* **2000**, *39*, 5707–5716; b) H. C. Kang, A. W. Hanson, B. Eaton, V. Boekelheide, *J. Am. Chem. Soc.* **1985**, *107*, 1979–1985; c) C. Cohen-Addad, P. Baret, P. Chautemps, J.-L. Pierre, *Acta Crystallogr., Sect. C* **1983**, *39*, 1346–1349; d) F. R. Heirtzler, H. Hopf, P. G. Jones, P. Bubenitschek, V. Lehne, *J. Org. Chem.* **1993**, *58*, 2781–2784; e) S. Kammermeier, P. G. Jones, I. Dix, R. Herges, *Acta Crystallogr., Sect. C* **1998**, *54*, 1078–1081; f) J. Powell, A. Lough, T. Saeed, *J. Chem. Soc., Dalton Trans.* **1997**, 4137–4138; g) M. Munakata, L. P. Wu, G. L. Ning, T. Kuroda-Sowa, M. Maekawa, Y. Suenaga, N. Maeno, *J. Am. Chem. Soc.* **1999**, *121*, 4968–4976.
[17] M. Cano, J. V. Heras, M. Maeso, M. Álvaro, R. Fernández, E. Pinilla, J. A. Campo, A. Monge, *J. Organomet. Chem.* **1997**, *534*, 159–172.
[18] S. Braun, H.-O. Kalinowski, S. Berger, *150 and More Basic NMR Experiments*, Wiley-VCH, Weinheim, **1998**.
[19] G. M. Sheldrick, *SHELXTL, Program for refinement of Crystal Structure*, University of Göttingen, Göttingen, Germany, **1997**.
[20] M. Nardelli, *J. Appl. Crystallogr.* **1995**, *28*, 659–659.

Received: March 17, 2005
Published Online: September 12, 2005

  